# EFFECT OF STRAIN RATE ON THE TENSILE FAILURE OF WOVEN REINFORCED POLYESTER RESIN COMPOSITES

L. Welsh, J. Harding

JOURNAL DE PHYSIQUE
Colloque C5, supplément au n°8, Tome 46, août 1985 

# EFFECT OF STRAIN RATE ON THE TENSILE FAILURE OF WOVEN REINFORCED POLYESTER RESIN COMPOSITES

L.M. Welsh and J. Harding

*Department of Engineering Science, University of Oxford, Parks Road, Oxford OX1 3PJ, U.K.*

Résumé - Des courbes contrainte-déformation déterminées en traction à des vitesses de $\sim 10^{-4}$, 10 et $1000 s^{-1}$ sur les composites renforcés par des tissus de carbone, Kevlar ou verre sont présentées. On détermine les variations du module de la contrainte et de la déformation à rupture en fonction de la vitesse de déformation. A l'inverse du comportement des composites carbone et Kevlar, on observe dans le cas des composites renforcés par fibre de verre un changement de mode de rupture à grande vitesse de déformation.

Abstract - Tensile stress-strain curves are obtained at strain rates of $\sim 10^{-4}$, $\sim 10$ and $\sim 1000/s$ for carbon, Kevlar and glass fibre woven-reinforced polyester resin composites and the variation of modulus, tensile strength and fracture strain with strain rate is determined. A change in the failure mode at the highest strain rates is observed for the glass but not the carbon or Kevlar reinforced composites.

## I - INTRODUCTION

The increasing use of fibre-reinforced plastics in situations involving dynamic loading, their developing application in energy absorbing systems associated with impact and their susceptibility to micro-damage under sub-critical impact, leading to a subsequent deterioration in mechanical properties at conventional loading rates, has resulted in an urgent need for fundamental studies of the effect of the rate of loading both on the mechanical strength and on the mechanisms of energy absorbtion in these materials. Unfortunately much of the previous work in this area has used Charpy or Izod type impact bend tests where stress-wave reflections and the complex modes of failure involved inhibit any fundamental analysis of the material response and of the effect of loading rate on the fracture behaviour. Although an instrumented tup may be used and load-time records obtained, allowing estimates of both the energy absorbed at the initiation of fracture and of the total work of fracture (1,2) to be made, the stress system under which failure occurs is complex and a fundamental study of material response is not possible. Other types of test which have been used include those employing a drop weight (3), where stress oscillations on the load cell signal obscured the details of the process and limited the maximum loading rate, and those employing a pendulum (4) or flywheel (5) to apply a direct tensile impact. In both these latter methods doubt remains regarding the accuracy of the strain measuring technique, which is particularly important when testing materials with such relatively low strains to failure.

In the second of these, the method developed by Kawata et al. (5), a version of the split Hopkinson's Pressure bar is employed. This technique, although widely used for the impact testing of metallic specimens, presents some difficulties when applied to composite materials, particularly as regards the design of the specimen. Recommended specimen designs for the uniaxial quasi-static testing of composite materials (6) are not suitable for use in the Hopkinson-bar (7). This problem has, to some extent, been avoided in tests using shear loading configurations (8, 9) but the greatest difficulty has been experienced in obtaining reliable data for impact tension. However,

in a recent paper (10) a newly developed technique for the tensile impact testing of fibre-reinforced composites, based on a modified version of the standard tensile split Hopkinson's pressure bar (SHPB), has been described. Results were presented for unidirectionally-reinforced CFRP, for which no effect of tensile strain rate was observed on the modulus, failure strength or fracture appearance over some seven orders of magnitude, and, in a subsequent paper (11), for woven-reinforced GFRP, where the modulus and failure strength both increased with strain rate and there was a marked change in the fracture appearance. Examination of the broken specimens showed considerable matrix damage preceding final fracture in the GFRP tests but not in those on CFRP specimens. A tentative phenomenological description of failure in woven GFRP specimens was proposed. This related (i) the rate dependence of the modulus to the effect of the epoxy resin matrix resisting the straightening of the axially-aligned rovings under increasing load, (ii) the subsequent reduced stiffness ('knee effect') to cracking in the matrix and a breakdown of the bonding between the matrix and the reinforcement and (iii) the rate dependence of the fracture strength and failure strain to the increased strength of glass fibres at impact rates allowing a greater degree of straightening before final failure. In contrast, the strain-rate independent behaviour of the CFRP specimens was related to the unidirectional nature of the reinforcement, where the straightening mechanism no longer applies, and an apparent rate insensitivity of the fracture strength of carbon fibres. In these preliminary tests, however, a direct comparison between the impact response of carbon and glass-fibre reinforced composites was not possible because of the different reinforcement geometries in the two composites studied.

Nevertheless, it follows from the above interpretation of these preliminary results that a CFRP specimen with a woven-reinforcement geometry might show both a rate dependent tensile modulus and an increasingly non-linear stress-strain response at high rates, provided the resistance of the matrix to the straightening of the carbon fibres contributes significantly to the total load carried by the specimen. However, a rate dependence of the fracture strength, if it depends only on the fibre properties, would not be expected. To investigate these possibilities, tests have been performed at tensile strain rates of $\sim 0.0001$/s, $\sim 10$/s and $\sim 700$/s on CFRP specimens with a satin-weave reinforcement geometry in a polyester resin matrix. To allow a direct comparison of the effect of the type of reinforcing fibre on the strain-rate senstiivity of fibre-reinforced plastics, similar tests have also been performed on KFRP and GFRP specimens with the same satin-weave reinforcement geometry and the same polyester resin matrix. The effect of strain rate on the tensile modulus, fracture strength and fracture strain is determined for the three types of specimen and the modes of failure are examined.

## II - EXPERIMENTAL DETAILS

Since the impact testing technique has been fully reported elsewhere (11) only a brief description will be given here. Thin strip specimens, waisted in the thickness direction, as shown in fig. 1, are fixed with epoxy adhesive in parallel-sided slots in the yoke and the inertia bar, see fig. 2. Strain gauges mounted on the inertia bar monitor both the stress transmitted by the specimen and the velocity at the upper end. A calibration for the velocity at the lower end of the specimen is obtained for a given impact velocity by the technique described previously (11) and the strain determined using the SHPB analysis. Signals from the inertia bar and specimen strain gauges were stored in a Datalabs type 922 transient recorder and subsequently displayed on an oscilloscope, hard copy being obtained on an X-t chart recorder. Typical oscilloscope traces for the inertia bar strain gauge signals in impact tests on the three types of composite are shown in fig. 3, the total sweep time being 100 μs. Comparative tests at low and intermediate rates were obtained on the same design of specimen using a standard screw-driven Instron loading machine, for a strain rate of $\sim 0.0001$/s, and a hydraulically-operated loading machine, for a strain rate of $\sim 10$/s. In at least one test at each strain rate on each type of specimen a check of the strain in the elastic region, and hence a confirmation of the specimen modulus, was made using strain gauges attached directly to the specimen. Typical traces, as displayed subsequently on an oscilloscope screen, for a test on a GFRP specimen in the hydraulic machine are shown in fig. 4.

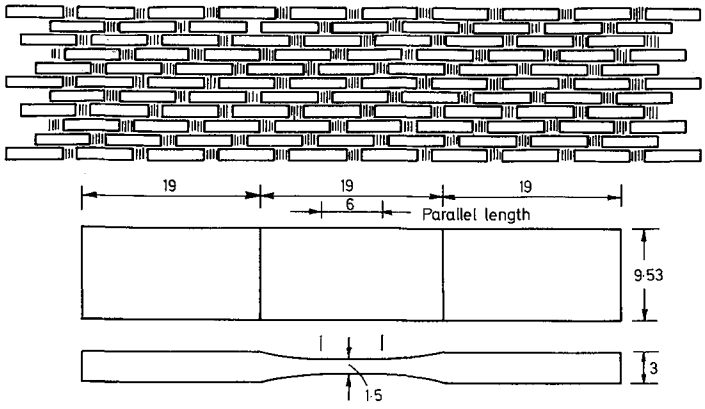


Fig.1 SPECIMEN DESIGN AND REINFORCEMENT CONFIGURATION
(all dimensions in millimetres)

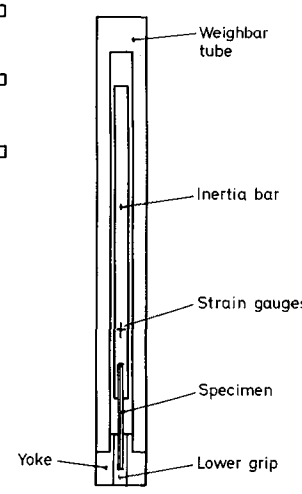


Fig.2 TENSILE SHPB

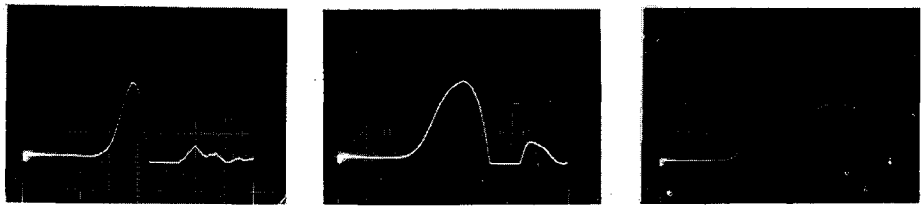

a) CFRP b) KFRP c) GFRP

Fig.3 INERTIA-BAR STRAIN GAUGE SIGNALS FOR IMPACT TESTS
(total sweep time - 100μs)

The total sweep time was 4 milliseconds. The upper trace was derived from the strain gauges attached directly to the parallel region of the specimen gauge length.

## III - SPECIMEN MATERIALS

Specimens were cut from 3mm thick laminates supplied by Fothergill and Harvey Ltd. Each laminate consisted of 8 reinforcement layers press moulded in Crystic 272 polyester resin to give a calculated volume fraction of 40%. A 5-end satin weave construction was used for each fabric with 6.7 tows/cm in both warp and weft directions for the Kevlar and the glass fabrics and 7.0 tows/cm for the carbon fabric, with corresponding fabric weights of 219.4, 353 and 283 g/m$^2$ respectively. The fibres were, respectively, kevlar 49 (type 968), E-glass (EC13) and Toray type T300-3000 filament carbon tows. The reinforcement geometry of the three types of specimen is shown, to the same scale as the specimen, in fig.1. Within the reduced specimen gauge thickness there are 4 layers of fabric while across the full width of the specimen there are contained between 6 and 7 longitudinal tows. This relatively coarse reinforcement geometry, in relation to the specimen dimensions, was dictated by the use of 3000 filament carbon tows in the woven carbon fabric due to the difficulty of obtaining carbon fabrics woven from the finer 1000 filament tows. It compares with the plain weave GFRP composite tested in the earlier work (11) where, for similar specimen dimensions, there were 9 layers of fabric in the specimen gauge thickness direction and 18 tows across the full width. In consequence an increased experimental scatter may be expected in the present tests. Although this could have been limited by increasing the specimen dimensions in proportion to the scale of the reinforcement geometry a corresponding increase in the stress-wave transit time across the specimen would introduce errors into the Hopkinson bar analysis in the elastic region.

## IV - RESULTS

### Stress-Strain Curves

Stress-strain curves for the CFRP specimens are presented in fig. 5 for 4 tests at each of 3 strain rates, nominally 0.0001/s, 10/s and 700/s. In all tests some inelastic deformation of the specimen was observed beyond the region of approximately linear stress-strain response. At the quasi-static loading rate audible cracking of the specimen was noticed at around the limit of the linear elastic region. Wide differences in the stress levels associated with the subsequent inelastic deformation are apparent when the 4 specimens tested at any given strain rate are compared. As discussed in the previous section this behaviour is thought to represent genuine differences in response between the various specimens due to the relatively coarse nature of the woven reinforcement geometry in relation to the overall specimen dimensions. It is not possible, therefore, to describe the mechanical behaviour of the composite in terms of a mean, or average, stress-strain curve at a given strain rate. Instead, the results have been characterised by determining, for each test, the initial slope (or tensile elastic modulus, E), the maximum stress supported by the specimen, (or tensile strength, $\sigma_m$), and the strain to fracture, $\varepsilon_f$, defined as the strain corresponding to the maximum stress. Despite the wide scatter it is clear that there is a significant increase in the maximum stress supported by the specimens at the impact loading rate and that this is accompanied by an increase in the linear elastic range. A wide scatter is also apparent in the strain to fracture at each strain rate such that the apparent slight increase in fracture strain at intermediate strain rates is probably not significant. Taking all the CFRP tests together, however, the average fracture strain, 1.59%, is significantly greater than that for unidirectionally reinforced specimens, $\sim$0.9%, determined in the earlier investigation (10).

Stress-strain curves for the KFRP specimens are presented in fig. 6 at the same three nominal strain rates. The behaviour is very similar to that shown by the CFRP specimens with again considerable scatter in the stress levels corresponding to the region of inelastic deformation but, despite this, again a clearly marked increase in the maximum stress at the impact loading rate. At all testing rates the failure strains for KFRP specimens exceeded those for the CFRP specimens but with a trend in the KFRP specimens for the failure strain to decrease slightly, but continuously, with increasing strain rate.

A markedly different behaviour is found, however, when the stress-strain curves for GFRP specimens, presented in fig. 7, are examined. These show a very significant increase in both the maximum stress and the fracture strain between the quasi-static and the intermediate rate tests. At the intermediate strain rate the stress-strain curve shows a very pronounced 'knee effect' with a much reduced stiffness at strains from $\sim$2%, the limit of the linear elastic region, up to failure at $\sim$7%. However, on increasing the strain rate further, to just over 1000/s, a change in behaviour is observed. The maximum stress is now reduced and corresponds to the stress level at the limit of the linear elastic region. Subsequent deformation is at an approximately constant or slightly decreasing load to a sufficiently high strain that failure was not reached in the standard sweep time of 100$\mu$s, see fig. 3c. In one impact test on a GFRP specimen the sweep time was increased to 200$\mu$s. Although this reduced the accuracy of calculation in the low strain elastic region it did allow the entire loading history to be recorded. In this test the fracture strain was calculated to be $\sim$13%

### Fracture Appearance

Despite the apparently increased extent of inelastic deformation shown by CFRP specimens at the intermediate loading rate no effect of strain rate on the fracture appearance could be detected. At all strain rates specimens broke in the central region of the gauge section, see fig. 8a. This figure also shows how the fracture surface is related to the reinforcement geometry. The inelastic deformation at high loads is clearly related to the long pull-out lengths of the fibre tows, more easily seen when the specimen of fig. 8a is viewed in silhouette, as in fig. 8b. This behaviour may be compared with that found in the earlier work on unidirectionally-reinforced CFRP (Hyfil) where again the fracture appearance was unaffected by strain rate but the pull-out lengths

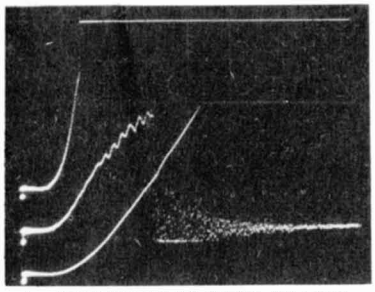


Fig.4 HYDRAULIC MACHINE TRACES
GFRP Test: sweep time, 4ms
a) Specimen strain
b) Specimen load
c) Crosshead displacement

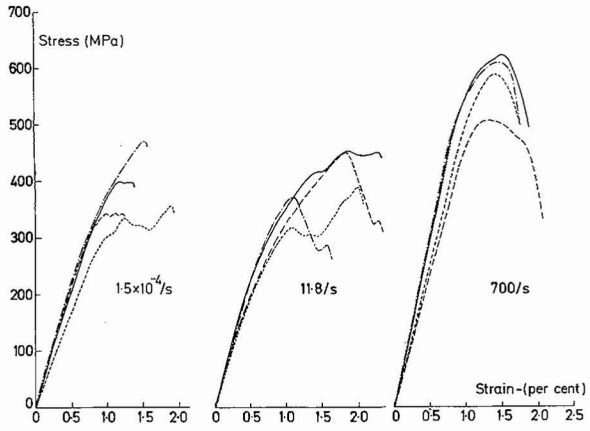


Fig.5
CFRP STRESS-STRAIN CURVES

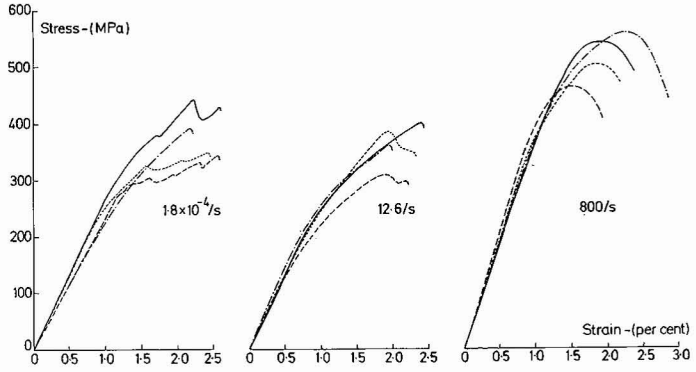


Fig.6
KFRP STRESS-STRAIN CURVES

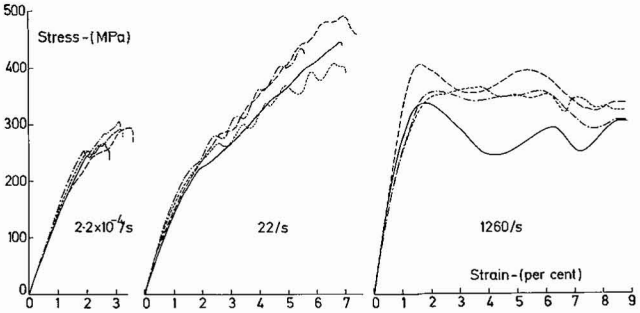


Fig.7
GFRP STRESS-STRAIN CURVES

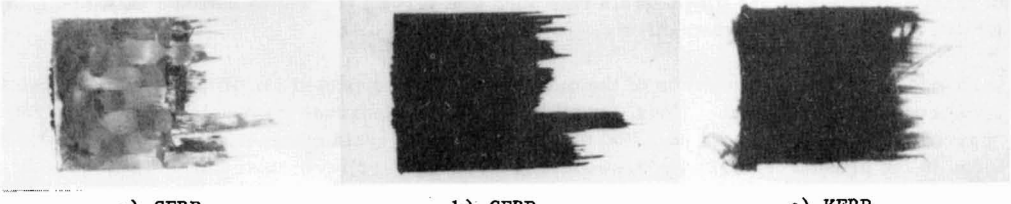

a) CFRP (reflected light: x3)
b) CFRP (transmitted light: x3)
c) KFRP (transmitted light: x3)

Fig.8 FRACTURE APPEARANCE OF CFRP AND KFRP SPECIMENS

were very short and the stress-strain response was near to linear-elastic through to failure. Examination of broken KFRP specimens also showed the fracture appearance to be rate independent. Although fracture strains were marginally higher than for CFRP, pull-out lengths were a little shorter, see fig. 8c. However, this may be a somewhat misleading observation since, although the pulled-out fibre tows of CFRP (and GFRP) were stiff and brittle, those of KFRP were soft and flexible and there was some indication that the polyester resin had not wetted-out the Kevlar fibres very well so that the measured mechanical properties for the KFRP specimens reflected more closely the behaviour of dry Kevlar fibres.

As in the earlier work (11), and unlike the behaviour of CFRP and KFRP described above, a marked effect of strain rate on the fracture appearance of GFRP specimens was observed. At the quasi-static rate, see fig. 9a, the main tensile fracture was at one end of the parallel gauge section with several pulled-out fibre tows extending into the tapered region but not as far as the grip region of the specimen, i.e. not within the parallel-sided slot of the loading-bar. Fibre tows will have also pulled-out from the half of the specimen shown in fig. 9a. At the intermediate loading rate the main tensile fracture again occurred, in the case shown in fig. 9b, just within the specimen parallel gauge region, but there were both a greater number of fibre tows pulling out and a markedly increased average pull-out length. The longest of the pulled-out fibre tows extended throughout the whole of the parallel gauge section, the whole of the tapered section and a further few millimetres into the region within the loading bar slot. On further increasing the strain rate to $\sim$1000/s, in the impact machine, a change in fracture mode was observed, see fig. 9c. The specimen disintegrated into three pieces as the central portion remained intact but pulled-out from the two ends which were still attached to the loading bars. When these end-pieces were cut off from the loading bars they each separated into two halves representing the tapered regions either side of the central pulled-out region. The longest pulled-out fibre tows extended at one end as far as the end surface of the original specimen. All other longitudinal tows failed in tension at some point in the tapered or grip regions. No clear tensile fracture surfaces were apparent at either end of the central region which was longer viewed from one side, 18.8mm or about 12 fibre tows, than viewed from the other, 6mm or about 4 fibre tows.

## V - DISCUSSION

### Effect of Strain Rate on the Tensile (Youngs) Modulus

The variation of Youngs modulus with strain rate for the three composites is shown in fig. 10. The experimental accuracy with which the modulus can be measured in the tensile testing techniques used here has been discussed previously (11) and is expected to be about ±5%. The much greater scatter here, of the order of ±15% in the CFRP tests, is thought to be related to the coarseness of the reinforcement geometry, as suggested in section III. Nevertheless, despite the scatter in the results of the CFRP tests a remarkably close agreement is apparent in the strain rate dependence of the tensile modulus for the three materials. Since the reinforcement geometry and the matrix resin are the same for all three composites, this gives strong support to the earlier proposal that the rate dependence of the modulus in woven-reinforced composites derives from the elastic interaction between the axially-aligned fibre tows and the resin matrix and depends on the rate-sensitivity of the matrix. The only difference between the three composites tested here is in the type of reinforcing fibre. This leads to the different absolute values of tensile modulus at any given strain rate such that $E_G < E_K < E_C$ where suffixes G, K and C denote GFRP, KFRP and CFRP respectively.

change in the rate-dependence of the modulus might be expected for different matrix resins or reinforcement geometries. Thus, for GFRP, a greater increase in modulus with strain rate was apparent in the earlier tests on a fine plain-weave epoxy resin composite, see fig. 11, than was found in the present tests on a coarse satin-weave polyester resin material. This is in accord with the greater elastic interaction that would be expected between the matrix resin and a fine plain-weave than a coarse satin-weave reinforcement geometry. Since the fibre volume fractions for the two types of GFRP were very similar, the difference in absolute modulus values in fig. 11 is presumably related to the different properties of the two matrix resins.

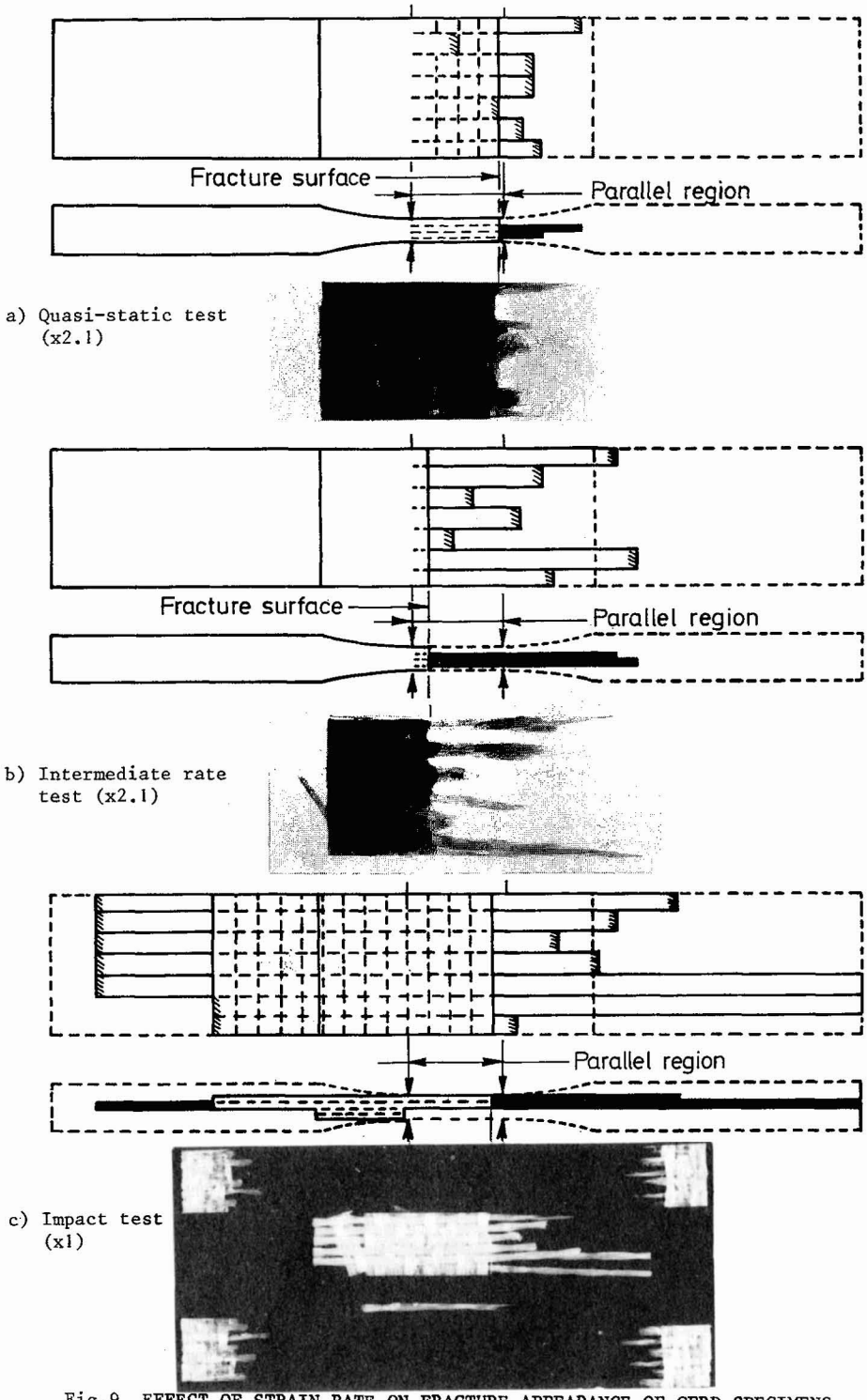


Fig.9 EFFECT OF STRAIN RATE ON FRACTURE APPEARANCE OF GFRP SPECIMENS

Effect of Strain Rate on the Tensile Strength

The variation of the tensile strength with strain rate for the CFRP and KFRP specimens is shown in fig. 12. Again the experimental scatter is quite large. Nevertheless both composites clearly show very similar behaviour with a nearly rate-independent strength of ∿400MPa up to a strain rate of ∿10/s and then a small, but significant, increase in strength, by about 25%, as the strain rate is raised to the order of 1000/s, the KFRP having a marginally lower strength than the CFRP. Previously it was assumed that the fracture strength of carbon fibres was rate independent. If the present increase in tensile strength at impact strain rates is not due to an increased strength of the carbon (and the Kevlar) fibres it suggests that the resin itself carries a significant proportion of the total load in woven reinforced specimens at the highest strain rates. This could be the case, provided the bonding between the resin and the reinforcement remains largely intact so that the elastic interaction between them is still possible. The observation that the fracture strains for CFRP and KFRP are relatively insensitive to strain rate and perhaps decrease slightly at the highest rates lends support to this proposition.

In previous work on woven GFRP (11), see fig. 13, a much greater rate-sensitivity of the tensile strength was observed, an increase of ∿70% being recorded between the quasi-static and intermediate rates of strain and an overall increase of ∿160% between the quasi-static and the impact rates of strain. The present results also show a significant rate sensitivity between $10^{-4}$ and 10/s, the tensile strength increasing by ∿50%. In the impact tests, however, this behaviour is reversed, the tensile strength showing a decrease of ∿25%. This corresponds to the apparent change in failure mode previously noted. Even with this change, however, the majority of the axially-aligned fibre tows in the impact loaded specimen of fig. 9c still failed in tension. Thus the tensile strength of woven reinforced GFRP would not seem to be solely determined by the rate-dependent fracture strength of the glass. In the present case the extra factor which may determine the response at the highest rates of strain is the ease with which fractured fibre tows may debond from the matrix over considerable distances from the point of failure so that fractures across individual fibre tows at widely separated sites in the specimen may nevertheless contribute to the final overall failure of the specimen. The other significant difference between the present and the earlier results for woven reinforced GFRP is in the effect of strain rate on the strain to fracture. Results for the rate dependence of the fracture strain are compared in fig. 14 for the various types of composite. Within the experimental scatter $\varepsilon_f$ for the satin-weave CFRP specimens is independent of strain rate over the entire range, $10^{-4}$ to $10^3$/s, while for satin-weave KFRP $\varepsilon_f$ shows a slight decrease from ∿2.5% to ∿2%. Both types of GFRP, however, show an increasing $\varepsilon_f$ with strain rate. For fine plain-weave material the increase is modest, from ∿1.8% to ∿2.7% but for the coarse satin-weave specimens it is dramatic, from ∿3% in quasi-static tests to ∿6.5% at intermediate rates while at impact rates $\varepsilon_f$>9% and in the one test for which it could be determined was found to be ∿13%. In both types of GFRP the extent of damage to either side of the fracture surface increased with increasing strain rate but the effect was more marked for the coarse satin-weave reinforcement geometry. Since, in principle, a fine plain-weave fabric should be capable of a greater extension on straightening than one of coarse satin-weave construction, the higher fracture strains in the latter must be due, at least in part, to the greater extent of the damage zone. However, even if the axially-aligned fibres in the satin-weave fabric were to fully straighten under tensile load, the maximum possible extension resulting would still only give a strain of ∿10%. In the impact tests, therefore, the overall failure strain must include a shear contribution resulting from pull-out of fibre tows. This implies that the near constant load in impact tests on satin-weave GFRP at strains greater than 2% is a measure of the force required to pull out the fibre tows at these very high rates.

In the light of the foregoing discussion the following general description of the fracture behaviour of the satin-weave GFRP specimens is proposed. At low and intermediate rates, where clear tensile fracture surfaces are observed, the tensile strength is determined by the rate-dependent fracture strength of the glass fibre tows and most fibre fractures contributing to final failure are in a restricted region of the specimen close to the resulting fracture surface. At impact rates, however, where no clear tensile fracture surfaces are observed, the fracture behaviour is controlled by pull-out of fibre tows leading to a high value of fracture strain. The tensile strength

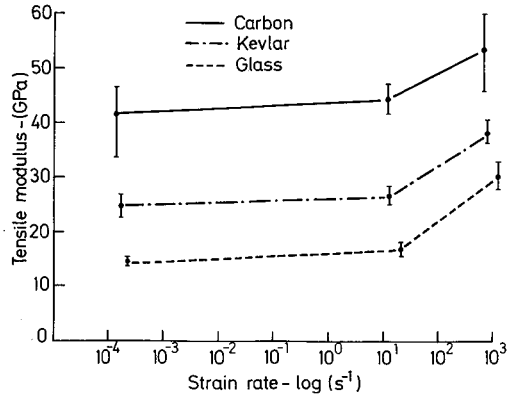


Fig.10
STRAIN-RATE DEPENDENCE OF TENSILE MODULUS
(present investigation)

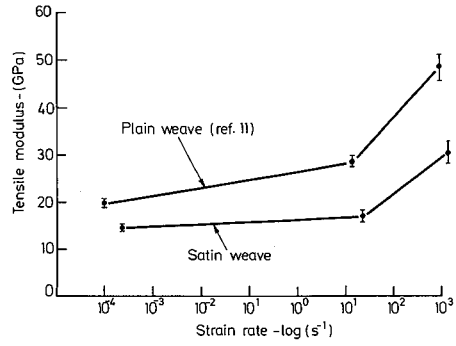


Fig.11
STRAIN-RATE DEPENDENCE OF TENSILE MODULUS
(woven GFRP specimens)

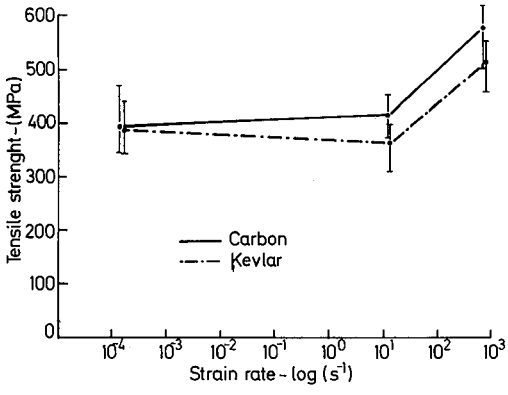


Fig.12
STRAIN-RATE DEPENDENCE OF TENSILE STRENGTH
(CFRP and KFRP specimens

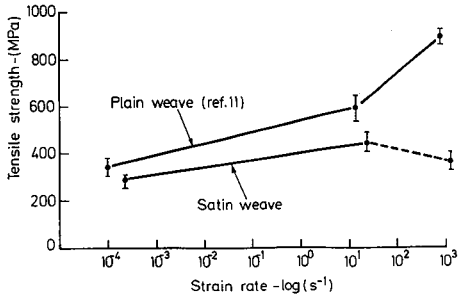


Fig.13
STRAIN-RATE DEPENDENCE OF TENSILE STRENGTH
(woven GFRP specimens)

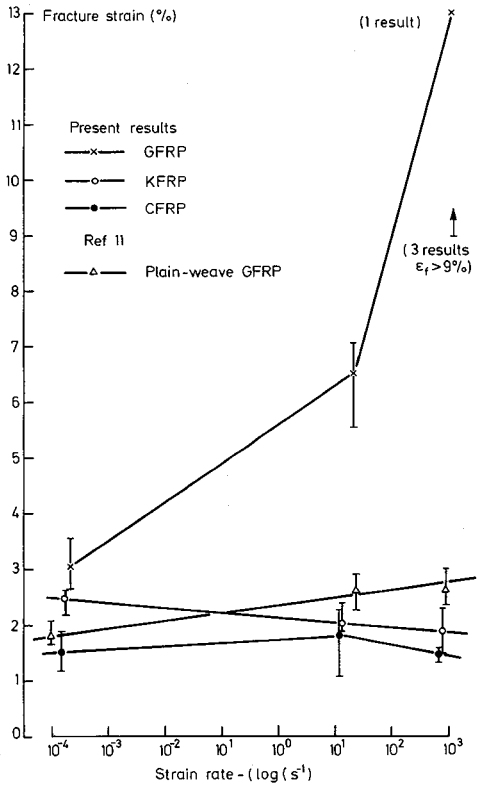


Fig.14
STRAIN-RATE DEPENDENCE OF FRACTURE STRAIN

may still be determined by the rate-dependent fracture strength of the glass fibre tows but, because such fractures occurring almost anywhere in the specimen may contribute to the final failure, on average the weaker tows will all fail first giving a lower overall fracture strength than at intermediate rates where such fractures are limited to a more restricted region of the specimen. To account for the change in failure mode at impact rates it is assumed that debonding between fractured fibre tows and the matrix becomes easier with increasing strain rate. This is not unreasonable since polymeric resin matrices show a tendency to greater brittleness with increasing strain rate.

## VI - CONCLUSIONS

Tensile stress-strain curves have been obtained at strain rates of $\sim 10^{-4}$/s, $\sim 10$/s and $\sim 1000$/s for polyester resin specimens reinforced with the same 5-end satin-weave fabric using carbon, Kevlar or glass fibres. A closely similar rate-dependence of the tensile modulus is obtained for all three composites, supporting a previous suggestion that the rate-dependence of the tensile modulus in woven-reinforced composites derives from the elastic interaction between the reinforcement and the resin matrix and is determined by the rate-dependence of the matrix strength. A significant increase in tensile strength at impact rates in CFRP (and KFRP) tests, however, does not support earlier suggestions that the tensile strength of CFRP is determined solely by the rate-independent fracture strength of the carbon fibres and raises the possibility that, for the woven reinforcement configuration, the matrix may carry a not insignificant proportion of the total load. For the GFRP specimens a change in the fracture mode is observed, from that controlled by the rate-dependent fracture strength of the glass at low and intermediate rates to that controlled by resistance to pull-out of fibre tows at impact rates, the change in mode resulting from a greater tendency for debonding between fractured fibre tows and the resin matrix at the highest rates of strain.

## ACKNOWLEDGMENTS

Grateful acknowledgment is made to Fothergill and Harvey Ltd. for the supply of the composite materials, and to the Science and Engineering Research Council, for the award to one author (L. M. Welsh) of a research studentship.

## REFERENCES

/1/ Adams, D. F. and Miller, A. K., J. Mater. Sci. 11 (1976) 1697
/2/ Marom, G., Fischer, S., Tuler, F. R. and Wagner, H. D., ibid. 13 (1978) 1419
/3/ Rotem, A. and Lifshitz, J. M., Proc. 26th Annual Tech. Conf. SPI Reinforced Plastics/Composites Division (Society of Plastics Industry, New York, 1971) paper 10G
/4/ Hayes, S. V. and Adams, D. F., J. Testing and Evaluation, 10 No. 2 (1982) 61
/5/ Kawata, K., Hondo, A., Hashimoto, S., Takeda, N. and Chung, H.L., Proc. Japan-US Conf. on Composite Materials (Japan Society for Composite Materials, Tokyo, 1981) 2
/6/ Ewins, P. D., R.A.E. Technical Report No. 71217 (1971)
/7/ Bai, Y. and Harding, J., Proc. Int. Conf. on Structural Impact and Crashworthiness, (Imperial College, London, 1984) 2 482
/8/ Harding, J., Conf. on Mech. Props. at High Rates of Strain (Institute of Physics, London, 1979) 318
/9/ Parry, T. and Harding, J., Colloque International du CNRS No. 139 (OUEL Report No. 1365, 1981)
/10/ Harding, J. and Welsh, L. M., Proc. 4th Int. Conf. on Composite Materials (Japan Society for Composite Materials, Tokyo, 1982) 845
/11/ Harding, J. and Welsh, L. M., J. Mater. Sci. 18 (1983) 1810